© 1999 Nature America Inc. • http://structbio.nature.com

Crystal structure of the N-terminal, growth factor-like domain of Alzheimer amyloid precursor protein

Jamie Rossjohn[1], Roberto Cappai[2,3], Susanne C. Feil[1], Anna Henry[2,3], William J. McKinstry[1], Denise Galatis[2,3], Lars Hesse[4], Gerd Multhaup[4], Konrad Beyreuther[4], Colin L. Masters[2,3] and Michael W. Parker[1]

[1]The Ian Potter Foundation Protein Crystallography Laboratory, St. Vincent's Institute of Medical Research, 41 Victoria Parade, Fitzroy, Victoria 3065, Australia. [2]Department of Pathology, University of Melbourne, Parkville, Victoria 3052, Australia. [3]The Mental Health Research Institute of Victoria, Parkville, Victoria 3052, Australia. [4]ZMBH, The Center for Molecular Biology, The University of Heidelberg, D-69120 Heidelberg, Germany.

Amyloid precursor protein (APP) plays a central role in Alzheimer disease. A proteolytic-breakdown product of APP, called β-amyloid, is a major component of the diffuse and fibrillar deposits found in Alzheimer diseased brains. The normal physiological role of APP remains largely unknown despite much work. A knowledge of its function will not only provide insights into the genesis of the disease but may also prove vital in the development of an effective therapy. Here we describe the 1.8 Å resolution crystal structure of the N-terminal, heparin-binding domain of APP (residues 28–123), which is responsible, among other things, for stimulation of neurite outgrowth. The structure reveals a highly charged basic surface that may interact with glycosaminoglycans in the brain and an abutting hydrophobic surface that is proposed to play an important functional role such as dimerization or ligand binding. Structural similarities with cysteine-rich growth factors, taken together with its known growth-promoting properties, suggests the APP N-terminal domain could function as a growth factor *in vivo*.

Amyloid precursor protein (APP) exists as several different isoforms, as a result of alternative splicing of a single gene, in many tissues[1]. The predominant isoform in neuronal tissues is a 695-residue protein that consists of a large N-terminal extracellular region, a transmembrane region and a small cytoplasmic tail[2]. The cytoplasmic region possesses a number of properties consistent with the possibility that APP is a receptor involved in signal transduction. For example, this region binds to G-proteins[3] and to proteins containing a phosphotyrosine interaction/binding domain[4]. Amyloid precursor protein can be released from cells by the proteolytic action of secretases[1]. The function of APP after detachment from membranes is not known. The N-terminal head of APP is a well-characterized domain of the extracellular region and has been shown to stimulate neurite outgrowth[5] and regulate synaptogenesis[6]. Of particular interest is the observation that an antibody directed toward this domain stimulates G-protein and MAP kinase activity[7,8].

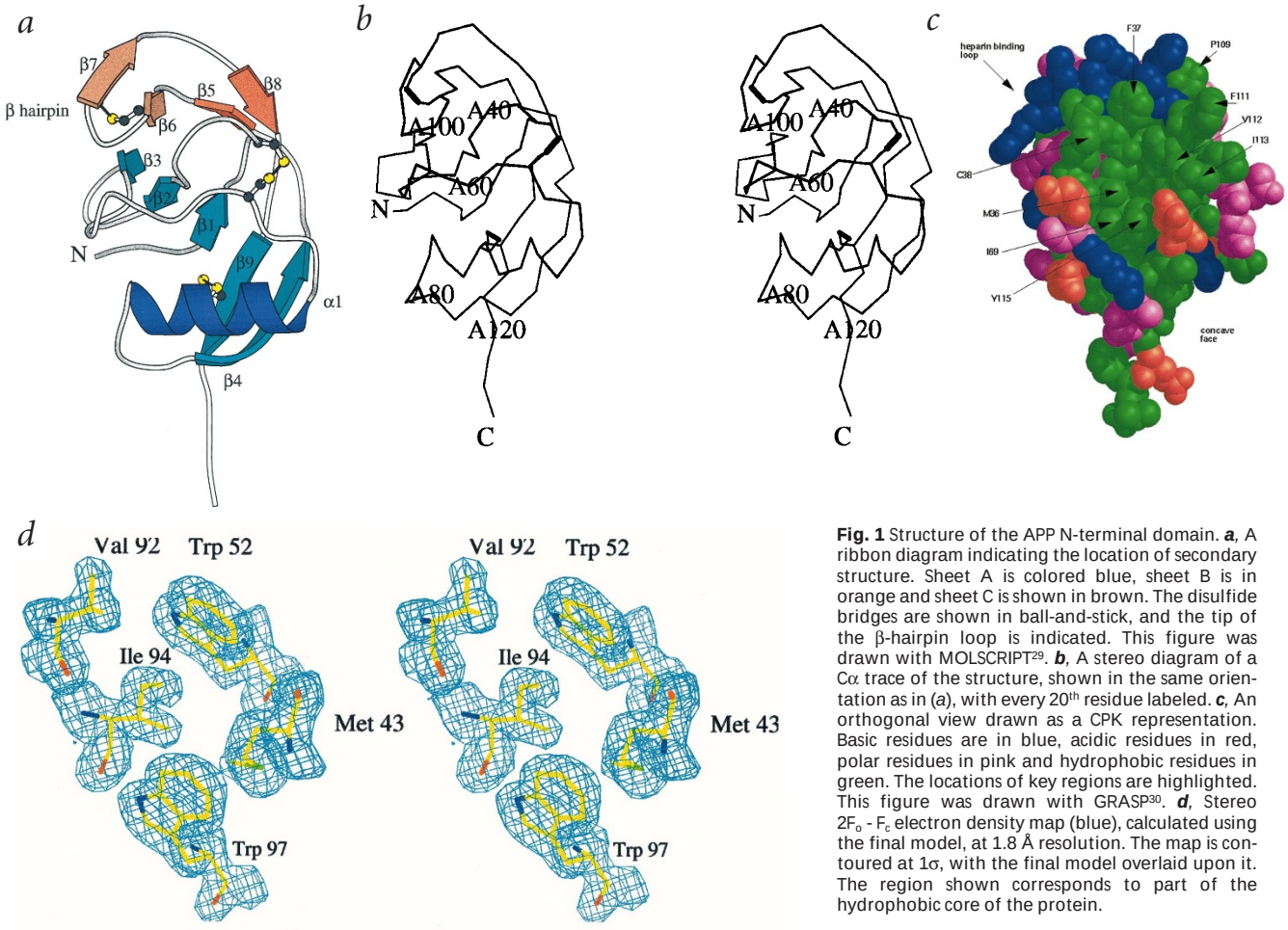

Fig. 1 Structure of the APP N-terminal domain. ***a***, A ribbon diagram indicating the location of secondary structure. Sheet A is colored blue, sheet B is in orange and sheet C is shown in brown. The disulfide bridges are shown in ball-and-stick, and the tip of the β-hairpin loop is indicated. This figure was drawn with MOLSCRIPT[29]. ***b***, A stereo diagram of a Cα trace of the structure, shown in the same orientation as in (*a*), with every 20th residue labeled. ***c***, An orthogonal view drawn as a CPK representation. Basic residues are in blue, acidic residues in red, polar residues in pink and hydrophobic residues in green. The locations of key regions are highlighted. This figure was drawn with GRASP[30]. ***d***, Stereo $2F_o - F_c$ electron density map (blue), calculated using the final model, at 1.8 Å resolution. The map is contoured at 1σ, with the final model overlaid upon it. The region shown corresponds to part of the hydrophobic core of the protein.

© 1999 Nature America Inc. • http://structbio.nature.com

© 1999 Nature America Inc. • http://structbio.nature.com

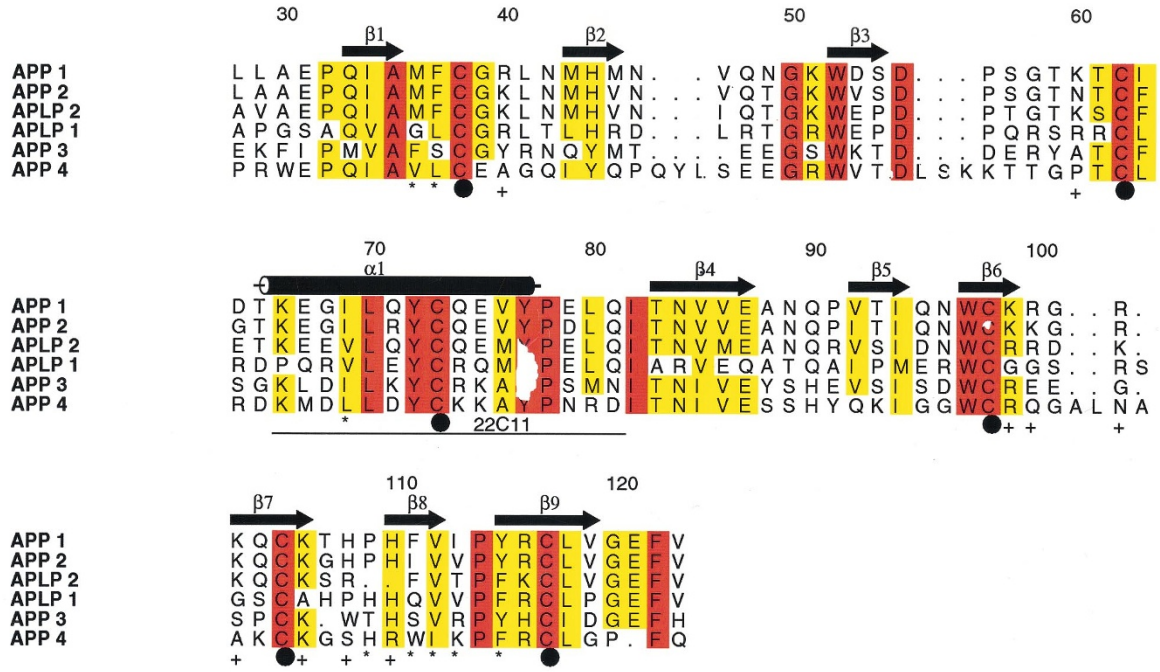

Fig. 2 Sequence alignment of the APP superfamily. The sequences were extracted from the SWISSPROT or GENBANK databases, aligned with AMPS and displayed with ALSCRIPT[31]. The secondary structure and residue numbering of human APP is shown above the alignment. Red boxes denote strictly conserved residues and yellow boxes denote either strictly conserved residues in all but one sequence or positions of conservative substitutions. The locations of cysteine residues are highlighted by the blackened circles and the epitope of the 22C11 monoclonal antibody[32] indicated. The positively charged residues of the heparin-binding surface are indicated by + and residues of the hydrophobic patch indicated with ✱. APP 1–4 are APPs from human, electric ray, *Caenorhabditis elegans* and *Drosophila.* APLP 1 and 2 are human APP-like homolog proteins.

© 1999 Nature America Inc. • http://structbio.nature.com

The antibody is presumably mimicking the action of a still-to-be-identified physiological ligand. Mutations in APP associated with hereditary Alzheimer disease also stimulate the same proteins, leading to the suggestion that the disease process may involve a breakdown in the regulation of APP-signaling function[8]. The N-terminal domain is cysteine-rich and contains a heparin-binding site[5]. Heparan sulfate proteoglycans may play a key role in Alzheimer disease pathogenesis: exogenous heparin induces APP production and amyloidogenic secretion[9], and a number of heparin-binding growth factors are expressed at increased levels in the brains of affected patients[10]. Recently, small heparin fragments have been proposed as possible drugs in preventing or retarding the disease[11]. In order to learn more about this critical domain, we have determined its three-dimensional structure by X-ray crystallography.

Overview of the structure

The structure of the APP N-terminal domain consists of nine β-strands (34% β-sheet) and one α-helix (12% helix) which fold into a compact, globular domain of dimensions 45 Å × 30 Å × 30 Å (Fig. 1*a*,*b*). Most of the strands are very short, with six of them comprising only three residues. At the core of the protein is a five-stranded antiparallel β-sheet (sheet A). The central sheet is covered on one side by two double-stranded sheets (sheets B and C) in a clamplike interaction and on the other side by the helix and a long loop. The helix represents the longest stretch of secondary structure, being 13 residues long. The domain possesses three disulfide bridges that act to tether parts of the protein together. The first disulfide (Cys 38–Cys 62) bridges a type II β-turn located between strands β1 and β2 and a loop preceding the helix; the second disulfide (Cys 73–Cys 117) bridges the helix to the C-terminal strand, β9; and the third disulfide (Cys 98 to Cys 105) links the strands, β6 and β7, of a β-hairpin. Amyloid precursor proteins from a variety of organisms have been sequenced (Fig. 2). Their respective N-terminal domains are well conserved with sequence identities ranging from 36% to 84%. The sequence alignments indicate that all the cysteine residues are strictly conserved and the hydrophobic core is well conserved suggesting the fold described here is maintained across the APP family.

Location of the heparin-binding site

An electrostatic calculation indicates there is a highly positively charged surface on one side of the domain that measures ~40 Å × 10 Å (Fig. 3). The region is centered about the disulfide, Cys 98 to Cys 105, and includes a peptide region, residues 96–110, that has previously been identified as part of a heparin-binding site[5]. Maintenance of the disulfide bridge is critical for neurite outgrowth[5] and activation of MAP kinase[12], suggesting the conformation of the loop is important. Residues that contribute to the positively charged surface include Arg 40, Lys 60, Lys 99, Arg 100, Arg 102, Lys 103 and Lys 106. There are also two histidine residues, His 108 and His 110, on the same surface. Surprisingly, few of these basic residues are conserved across the APP family (Fig. 2), even though other members bind heparin with similar affinity[13]. Nevertheless, the overall positive patch is conserved (Fig. 3). The size of the positive patch suggests that an octasaccharide fragment of heparin would provide optimal binding interactions with the domain. The surface is dominated by the β-hairpin loop (residues 96–110), which also represents the most

© 1999 Nature America Inc. • http://structbio.nature.com

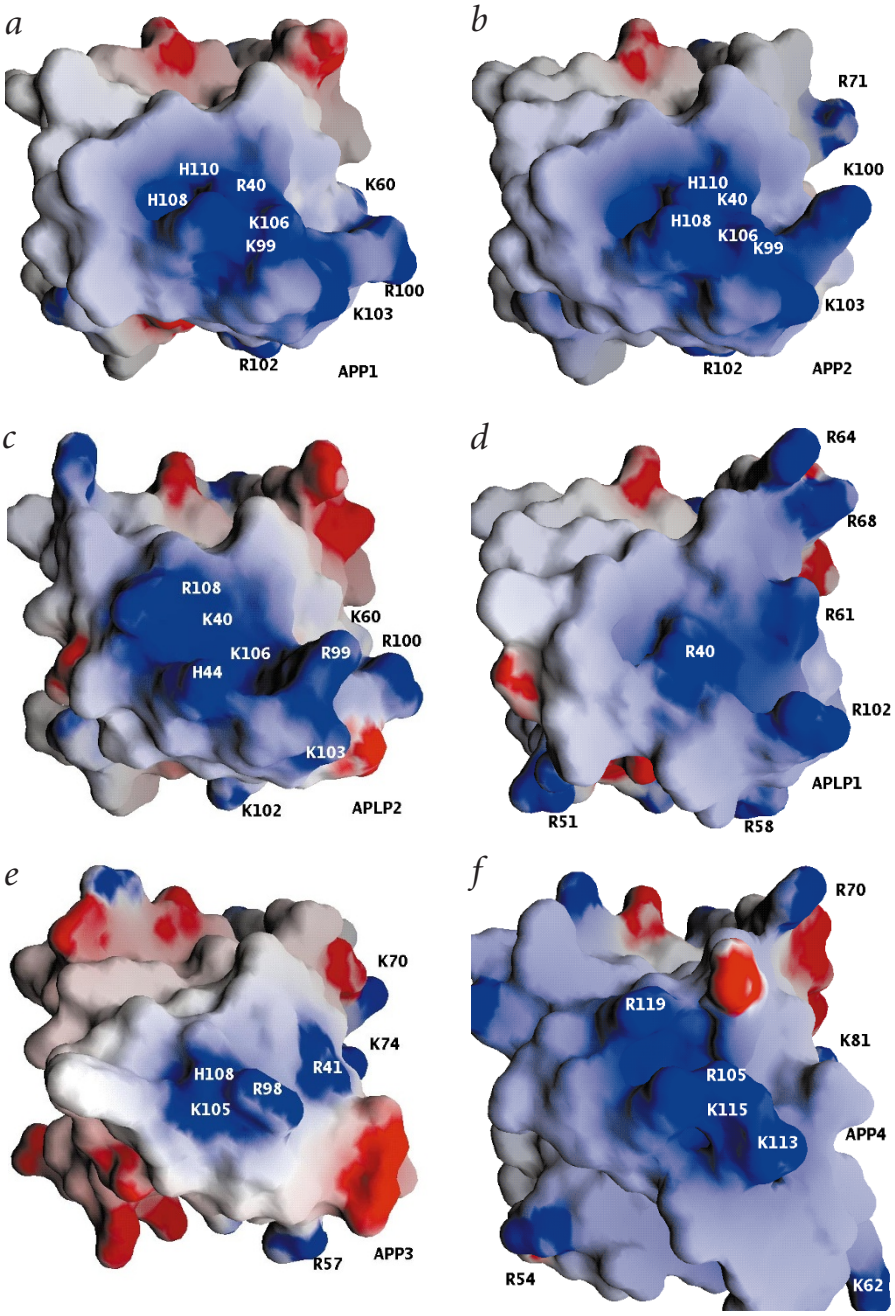

Fig. 3 Electrostatic surface representations[30] of APP family members. Blue indicates electropositive potential (> 10 kT) and red indicates electronegative potential (< -10 kT).

mobile region of the structure, with a mean temperature factor of 29.3 Å^2, compared to the mean for the whole molecule of 18.1 Å^2.

Surface hydrophobic patch

Surface hydrophobicity can play a key role in protein–protein interactions. Intriguingly, there is a large hydrophobic patch, of dimensions 20 Å × 20 Å, immediately adjacent to the heparin-binding region (Fig. 1*c*). The major contributors to this surface include Met 36, Phe 37, Ile 69, Pro 109, Phe 111, Val 112, Ile 113 and Tyr 115. The hydrophobicity of the surface is conserved across the APP family. We hypothesize that this surface may fulfill one or more of four possible functions. Amyloid precursor protein binds to both the carbohydrate and core protein of proteoglycans[14,15]. One possibility is that this surface provides binding specifity toward particular proteoglycans such as glypican (K_d = 2.8 nM) and perlecan, which are known to bind to this domain[14,16]. This notion is supported by the observation that the monoclonal antibody 22C11, which recognizes one edge of this surface, inhibits neurite outgrowth[17] and functional synapse formation[6]. Alternatively, the surface may compose part of the interface between the N-terminal domain and the metal-binding domain that immediately follows it in the primary structure. This possibility seems less likely since the hydrophobic surface is located far away from the C-terminus. Furthermore, the concave surface immediately adjacent to the C-terminus (Fig. 1*c*) is conserved between different APPs, suggesting it as a more likely candidate for the domain interface. A third possibility is that the hydrophobic patch is part of a dimerization interface. The signaling mechanism of many single-spanning receptors relies on receptor dimerization[18]. Furthermore, a number of growth factors are known to dimerize in the presence of heparin to form extended heparin-binding regions[19–21]. Finally, the 22C11 antibody that recognizes part of this surface (Fig. 2) appears to mimic the action of an unknown agonist ligand, since it stimulates G-protein and MAP kinase activity through the cytoplasmic tail of APP[7,8]. Intriguingly, since the antibody is a divalent IgG1 molecule, it is possible that the activation involves dimerization of APP through the N-terminal head.

Biological implications

The overall fold of the APP N-terminal domain can be classified as mainly β, a fold that includes a number of cysteine-rich growth factors (such as epidermal growth factor, tumor necrosis factor and nerve growth factor), but the APP domain does not resemble any of them or indeed, any other protein of known three-dimensional structure as judged by the program DALI[22]. However, like APP, a number of growth factors also possess disulfide-bonded, β-hairpin loops implicated in proteoglycan binding. These include midkine[19], hepatocyte growth factor (HGF)[20] and vascular endothelial growth factor[23]. In all cases the loop is long, flexible and highly charged with basic residues. These properties appear ideal for binding heparin oligosaccharides where the flexibility would allow induced-fit binding through the positively charged residues around the sulfate moi-

© 1999 Nature America Inc. • http://structbio.nature.com

© 1999 Nature America Inc. • http://structbio.nature.com

eties of the carbohydrate. There is further similarity between APP and HGF in the loop regions. The tips of the β-hairpin loops can be superimposed with a root-mean-square deviation of 2.4 Å over the Cα atoms of 10 residues. Furthermore, a structure-based sequence alignment of part of this region (residues 100–106 of APP and residues 91–97 of HGF) shows that residues at equivalent positions (RGRKQC of APP *versus* KARKQC of HGF) are either the same or represent conservative substitutions. In addition, the C-terminal position includes one of the cysteines of the loop disulfide. However, the close match is likely to be fortuitous as this region represents one of the most dissimilar stretches of sequence in the APP superfamily (Fig. 2), and the other cysteine of the loop disulfide is contributed by structurally different regions of each protein. The extracellular domain of APP has recently been shown to be a potent mediator of thyrocyte proliferation[24] and can potentiate the phosphorylation of the receptor tyrosine kinase, trkA, caused by nerve growth factor binding[25]. Presumably, the growth-promoting activity of APP is expressed after it is released from membranes through the action of secretases. In conclusion, the structural similarities to some growth factors, in concert with the known growth-promoting properties of APP[24,25] and its N-terminal domain[5,6,17], strongly indicate that $APP_{28–123}$ (residues 28–123) can be classified as a new member of the cysteine-rich growth factor superfamily.

Table 1 Crystallographic analysis[1]

a, Data collection and phasing statistics				
	Native 1	Native 2	$K_3UO_2(F)_5$	$SmCl_3$
Soak time (days)	–	–	2	28
Soaking concentrations (mM)	–	–	5	80
Temperature of collection (K)	290	100	290	290
Resolution limit (Å)	2.0	1.8	2.0	2.7
Observations	16,811	29,942	24,740	7,480
Unique reflections	7,063	9,710	10,981	2,701
Completeness (%)	96 (83)	99 (98)	97 (87)	86 (92)
Multiplicity	2.4	3.1	2.3	2.8
I/σ_I	11.1 (3.3)	28.3 (7.4)	8.4 (2.4)	7.2 (1.9)
No. of data $>2\sigma_I$ (%)	77 (65)	95 (87)	83 (60)	71 (58)
R_{merge} (%)[3]	10.4 (24.6)	3.2 (17.8)	7.7 (23.4)	12.9 (44.3)
$<\|F_H\|> / E$ (acentric / centric)[3]	–	–	1.2 / 1.0	1.0 / 0.8
Heavy-atom sites	–	–	1	1
R_{cullis} (acentric / centric)[4]	–	–	0.8 / 0.7	0.9 / 0.8
b, Refinement statistics				
Resolution range (Å)	8.0–1.8			
R-factor (%)[5]	20.3			
R_{free} (%)[5]	24.2			
Atoms in model				
Protein (nonhydrogen)	771			
Water molecules	120			
R.m.s. deviations from ideal				
Bond lengths (Å)	0.006			
Bond angles (°)	1.32			
Impropers (°)	0.66			
Dihedrals (°)	26.92			
Average atomic B-factors (Å^2)				
Main chain	16.4			
Side chain	19.7			
Water	31.6			

[1]The values in parentheses are for the highest resolution bin (approximate interval 0.1 Å).
[2]$R_{merge} = \Sigma_{hkl}\Sigma_i|I_i - <I>| / |<I>|$, where I_i is the intensity for the i^{th} measurement of an equivalent reflection with indices h,k,l.
[3]$<|F_H|> / E$ is a measure of the phasing power of the derivative where $<|F_H|>$ is the r.m.s. heavy-atom derivative structure factor amplitude, and E is the lack-of-closure error.
[4]$R_{cullis} = \Sigma||F_{PHC}| - |F_{PH}|| / \Sigma||F_{PH}| - |F_P||$. The summation is over all centric reflections. F_{PHC} and F_{PH} are calculated and measured derivative structure factor amplitudes, respectively. F_P is the native structure factor.
[5]R-factor = $100(\Sigma||F_o| - |F_c|| / \Sigma|F_o|$, using all data except 10%, which were used for the R_{free} calculation.

Methods

Crystallization and data collection. The expression, purification and crystallization of the APP growth-promoting domain will be described in detail elsewhere. Briefly, the construct, consisting of residues 18–350 from the APP_{1-770} isoform, was expressed and purified from *Pichia pastoris* as described[26]. The protein was concentrated to 10 mg ml^{-1} in 5 mM Tris-HCl buffer at pH 7.5. The best crystals were grown by the hanging-drop vapor diffusion method at 22 °C from 22% PEG 10K and 100 mM HEPES at pH 7.5. The crystals required approximately two weeks to grow to maximal size. N-terminal sequencing and mass spectrometry revealed that the crystals consisted of a proteolytic-breakdown product, residues 23–128. The crystals belong to space group $P2_12_12_1$ with cell dimensions a = 31.2 Å, b = 48.6 Å, c = 67.4 Å. There is one monomer in the asymmetric unit that corresponds to a solvent content of ~38%. All data were collected in-house on a MAR Research area detector with CuKα X-rays generated by a Rigaku RU-200 rotating-anode generator. The diffraction data were processed and analyzed using DENZO[27], SCALEPACK[27] and programs in the CCP4 suite (Daresbury Laboratory, UK) (Table 1).

Structure determination. The crystal structure was solved by multiple isomorphous replacement (Table 1). Crystals were soaked in artificial mother liquor containing the derivative at room temperature. One major site was located in the isomorphous difference Patterson of the uranyl fluoride derivative. The samarium site was found by cross-difference Fourier using phases derived from the uranyl SIR data. Anomalous scattering data were collected for both derivatives and were used to establish unequivocally the correct handedness of the structure. Heavy-atom parameters were refined and phases calculated using MLPHARE (CCP4 suite). The overall figure of merit was 0.31 (for the resolution shell 20.0–2.0 Å). The phases were subsequently improved using density modification with DM (CCP4 suite). The density-modified electron density map, calculated to 2.0 Å resolution, was readily interpretable with the help of skeletonized maps. The initial model was improved by five cycles of model building and refinement against native data collected from flash-frozen crystals (native 2 in Table 1) using the slow-cool protocol of X-PLOR (A.T. Brunger, Yale University, New Haven, CT, USA). Tightly restrained individual isotropic temperature factors were employed in the latter cycles of refinement.

Model quality. The final model comprises residues 28–123 (Table 1). The map interpretation was checked by examination with simulated-annealing omit maps from N- to C-terminus. The correctness of the tracing is also supported by the convincing fit of all 11 aromatic residues, the location of the two heavy-atom sites in chemically reasonable positions (the uranyl ion binds to Asp 53 and the samarium ion binds to Glu 87) and 3D–1D scores that never fell

© 1999 Nature America Inc. • http://structbio.nature.com

© 1999 Nature America Inc. • http://structbio.nature.com

below 0.2 (ref. 28). As expected from a high-quality 1.8 Å resolution map (Fig. 1*d*), the path of the polypeptide was clear and the side-chain density well defined. More than 90% of the residues fall in the most-favored region of the Ramachandran plot, and none fall in the disallowed regions (CCP4 suite).

Coordinates. Coordinates have been deposited in the Protein Data Bank (accession code 1MWP).

Acknowledgments

This work was supported by grants from the National Health and Medical Research Council of Australia to C.L.M. and M.W.P. K.B. is supported by the Deutsche Forschungsgemeinschaft and the Bundesministerium für Forschung und Technologie. J.R. is an Australian Research Council Postdoctoral Fellow, S.C.F. holds an International Centre for Diffraction Data Crystallography Scholarship and M.W.P. is an Australian Research Council Senior Research Fellow.

Correspondence should be addressed to M.W.P. *email: mwp@rubens.its.unimelb.edu.au*

Received 23 September, 1998; accepted 7 December, 1998.

1. Mattson, M.P. *Physiol. Rev.* **77**, 1081–1132 (1997).
2. Kang, J. *et al. Nature* **325**, 733–736 (1987).
3. Okamoto, T. *et al. EMBO J.* **15**, 3769–3777 (1996).
4. Zambrano, N. *et al. J. Biol. Chem.* **272**, 6399–6405 (1997).
5. Small, D.H *et al. J. Neurosci.* **14**, 2117–2127 (1994).
6. Morimoto, T., Ohsawa, I., Takamura, C., Ishiguro, M. & Kohsaka, S. *J. Neurosci. Res.* **51**, 185–195 (1998).
7. Okamoto, T., Takeda, S., Murayama, Y., Ogata, E. & Nishimoto, I. *J. Biol. Chem.* **270**, 4205–4208 (1995).
8. Murayama, Y. *et al. Gerontology* **42**, 2–11 (1996).
9. Leveugle, B. *et al. Neurochem. Int.* **30**, 543–548 (1997).
10. Fenton, H. *et al. Brain Res.* **779**, 262–270 (1998).
11. Leveugle, B. *et al. J. Neurochem.* **70**, 736–744 (1998).
12. Greenberg, S.M., Qiu, W.Q., Selkoe, D.J., Ben-Itzhak, A. & Kosik, K.S. *Neurosci. Lett.* **198**, 52–56 (1995).
13. Bush, A.I., Pettingell, W.H., de Paradis, M., Tanzi, R.E. & Wasco, W. *J. Biol. Chem.* **269**, 26618–26621 (1994).
14. Narindrasorasak, S. *et al. J. Biol. Chem.* **266**, 12878–12883 (1991).
15. Williamson, T.G., Nurcombe, V., Beyreuther, K., Masters, C.L. & Small, D.H. *J. Neurochem.* **65**, 2201–2208 (1995).
16. Williamson, T.G. *et al. J. Biol. Chem.* **271**, 31215–31221 (1996).
17. Ohsawa, I., Takamura, C. & Kohsaka, S. *Biochem. Biophys. Res. Commun.* **236**, 59–65 (1997).
18. Spencer, D.M., Wandless, T.J., Schreiber, S.L. & Crabtree, G.R. *Science* **262**, 1019–1024 (1993).
19. Iwasaki, W. *et al. EMBO J.* **16**, 6936–6946 (1997).
20. Zhou, H. *et al. Structure* **6**, 109–116 (1998).
21. DiGabriele, A.D. *et al. Nature* **393**, 812–817 (1998).
22. Holm, L. & Sander, C. *J. Mol. Biol.* **233**, 123–138 (1993).
23. Fairbrother, W.J., Champe, M.A., Christinger, H.W., Keyt, B.A. & Starovasnik, M.A. *Structure* **6**, 637–648 (1998).
24. Pietrzik, C.U. *et al. Proc. Natl. Acad. Sci. USA* **95**, 1770–1775 (1998).
25. Akar, C.A. & Wallace, W.C. *Mol. Brain. Res.* **56**, 125–132 (1998).
26. Henry, A., Masters, C.L., Beyreuther, K. & Cappai, R. *Protein Expr. Purif.* **10**, 283–291 (1997).
27. Otwinowski, Z. & Minor, W. *Methods Enzymol.* **276**, 307–326 (1997).
28. Lüthy, R., Bowie, J.U. & Eisenberg, D. *Nature* **356**, 83–85 (1992).
29. Kraulis, P.J. *J. Appl. Crystallogr.* **24**, 946–950 (1991).
30. Nicholls, A., Sharp, K.A. & Honig, B. *Prot. Struct. Funct. Genet.* **11**, 281–293 (1991).
31. Barton, G.J. *Protein Eng.* **6**, 37–40 (1993).
32. Hilbich, C., Mönning, U., Grund, C., Masters, C.L. & Beyreuther, K. *J. Biol. Chem.* **268**, 26571–26577 (1993).

© 1999 Nature America Inc. • http://structbio.nature.com

A *cis* proline turn linking two β-hairpin strands in the solution structure of an antibody-bound HIV-1_{IIIB} V3 peptide

Vitali Tugarinov, Anat Zvi, Rina Levy and Jacob Anglister

Department of Structural Biology, The Weizmann Institute of Science, Rehovot 76100, Israel.

The refined solution structure of an 18-residue HIV-1_{IIIB} V3 peptide in complex with the Fv fragment of an anti-gp120 antibody reveals an unexpected type VI β-turn comprising residues RGPG at the center of a β-hairpin. The central glycine and proline of this turn are linked by a *cis* peptide bond. The residues of the turn interact extensively with the antibody Fv. $^{15}N\{^1H\}$ NOE measurements show that the backbone of the peptide, including the central QRGPGR loop, is well ordered in the complex. The solution structure is significantly different from the X-ray structures of HIV-1_{MN} V3 peptides bound to anti-peptide antibodies. These differences could be due to a two-residue (QR) insertion preceding the GPGR sequence in the HIV-1_{IIIB} strain, and the much longer peptide epitope immobilized by the anti-gp120 antibody.

To date, the V3 loop is the only gp120 epitope found to be the target of numerous HIV-neutralizing antibodies[1]. Segments of V3 or its immediate vicinity form the binding site for the gp120 co-receptors on T-cells and macrophages[2,3], and its sequence determines the phenotype of the virus[4]. Escape of HIV-1 from the immune system is associated with the lack of specific anti-V3 antibodies *in vivo*[5]. Neutralization of a variety of HIV-1 strains has been shown with serum obtained after immunization with antigens containing V3 peptides of different strains[6,7]. The crystal structures of two anti-peptide HIV-neutralizing antibodies in complex with a synthetic peptide derived from the V3 loop of the HIV-1_{MN} (MN strain) gp120 were determined[8,9]. Most recently, the crystal structure of a CD4–gp120–antibody Fab complex was solved[10] with the V3 loop deleted from the gp120 construct to enable crystallization.

0.5β is a potent strain-specific HIV neutralizing antibody[11] that was raised against HIV-1_{IIIB} (IIIB strain) gp120 and protects chimpanzees from HIV-1 infection[12]. The affinity of 0.5β for the V3 peptide P1053 (RKSIRIQRGPGRAFVTIG) was found to be comparable to its affinity for the intact glycoprotein[13]. Recent NMR studies using the 0.5β antibody Fab fragment suggested that the antibody-bound peptide may adopt a β-hairpin conformation[14]. However, the lack of information on amide proton interactions and the molecular weight of the Fab fragment precluded exact definition of the peptide backbone conformation. Here we present conclusive NMR evidence that the peptide backbone folds into two anti-parallel β-strands linked by a six-residue loop comprising an unexpected type VI *cis* proline turn. The refined solution structure was obtained by NMR isotope filtering[15] using unlabeled P1053 complexed with the $^{13}C/^{15}N$-labeled 0.5β Fv fragment and isotope editing techniques using ^{15}N-labeled P1053 in complex with the unlabeled Fv.

Peptide resonance assignments and NOE interactions

The side-chain and α proton resonances of all the residues of P1053 bound to 0.5β Fab excluding those of Arg 8, Gly 12, Gly 14 and Arg 15 were assigned previously using difference spec-